Hardee
1978

I. Observational Properties of Pulsars

A) Pulsar Emission

1) Crab pulsar - period = .033 sec, radio, optical, x-ray and γ-ray emission, pulse and interpulse, all emission in phase except radio precursor to the main pulse.

2) Vela pulsar - period = .083 sec, radio, optical and γ-ray emission, no detectable x-ray emission at present sensitivity, single radio pulse preceeds two γ-ray pulses with two optical pulses between the γ-ray pulses.

3) Radio pulsars - on the order of 150 radio pulsars, two "typical" radio pulsars also γ-ray pulsars with periods on the order of .5 sec.

B) Properties of Integrated Radio Emission

1) Pulse window constructed by integrating over many pulses.

2) Spectra peak 50 - 1000 MHz integrated over many pulses, large variation pulse to pulse, in general steep decrease in luminosity on either side of peak.

3) Polarization of integrated pulse often shows steady change in position angle of linear polarization across pulse window

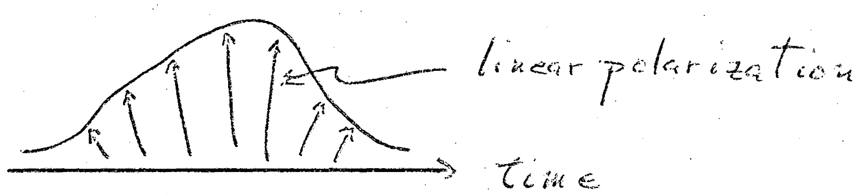

In general circular polarization is much smaller than linear polarization, sense of circular polarization may change through pulse.

C) Structure and Properties of Individual Pulses

1) Subpulses:

A single pulse may consist of several subpulses. Sometimes the position angle of linear polarization rotates 90 degrees at the boundary of subpulses. It also appears that the sense of circular polarization changes as linear polarization rotates. In some pulsars the subpulses drift across the pulse window. In general the position angle of linear polarization is a function of the position in the integrated pulse window except on the edges of a subpulse.

2) Micropulses:

Timescales - pulse period $\sim$ .5 sec, pulse window $\sim$ 50 msec, subpulse $\sim$ 5 msec, micropulse $\sim$ 50 μsec.

Behavior of linear and circular polarization similar to that seen for some subpulses, i.e., 90 degree change in position angle of linear polarization and change in sense of circular polarization at boundaries of micropulses. In general percentage of linear polarization very high, sometimes as high as 100 percent. Circular polarization sometimes as high as 50 percent.

II. Theory

A) Magnetosphere

We consider the case of an aligned rotator. In a vacuum

$$\underline{E} = - (\underline{v} \times \underline{B})/c = - 1/c\ (\underline{\Omega} \times \underline{R}) \times \underline{B}\ .$$

If the magnetic field is dipolar the resulting electric field is a quadrapole. The component of $\underline{E}$ parallel to $\underline{B}$ is

$$\underline{E} \cdot \underline{B} = \Omega R_s/c\ (R_s/R)^7\ B_s^2 \cos^3\theta$$

and at the stellar surface

$$\underline{E} \cdot \underline{B} = \Omega R_s/c\ (B_s^2 \cos^3\theta\ )$$

Strong electric field parallel to the magnetic field at the stellar surface. If particles accelerated from the surface then self consistent solution found from Maxwell's equations in corotating frame (note not inertial frame)

$$\nabla \cdot \underline{E} = 4\pi\ (\eta - \eta_R)$$

$$\nabla \cdot \underline{B} = 0$$

$$\nabla \times \underline{E} = - 1/c\ (\partial \underline{B}/\partial t)$$

$$\nabla \times \underline{B} = 4\pi/c\ (\underline{J} - \underline{J}_R) + 1/c\ (\partial \underline{E}/\partial t)$$

In the above

$$4\pi\ \eta_R = \nabla \cdot \underline{E} = \nabla \cdot (- 1/c\ (\underline{\Omega} \times \underline{R}) \times \underline{B})$$

and

$$\eta = J_s/v\ (B/B_s)$$

where J_s is steady current flow along the open magnetic field lines.
The electric field available for particle acceleration depends on the charge difference $\eta - \eta_R$.

The resulting particle flow will be:

(a) Space charge limited - particles pulled freely from the stellar surface limited by the charge difference.

(b) Vacuum gap - particle binding energy too high to be pulled from the stellar surface by the vacuum electric field.

Present calculations make it unclear as to which of the above will be the case. In either case the accelerating potential will be less than the maximum available

$$\Delta V_{Max} \sim 6.6 \times 10^{12} (B_s/10^{12})\ P^{-2} \text{ Volts}$$

because (a) $|\eta - \eta_R| < \eta_R$ or (b) gap breaks down in electron-positron pair production discharge when $\Delta V << \Delta V_{Max}$.

B) Curvature Radiation, Pair Production and γ-ray Emission

Charged particles traveling along curved magnetic field lines emit curvature radiation with peak emission at

$$\nu_c = 3\gamma^3/2\pi\ (c/\rho_c)$$

and

$$I_\nu \propto (\nu/\nu_c)^{1/3} \qquad \nu < \nu_c$$

where ρ_c is the radius of curvature. Near the stellar surface emission is primarily γ-rays. γ-rays with energies in excess of 100 Mev pair produce in the large magnetic field near the surface. Lower energy γ-rays can escape and may give rise to the observed pulsed emission at $\sim$50 Mev from the Vela and two typical radio pulsars. In a vacuum gap model of the magnetosphere pair production discharges (sparks) limit the potential drop across the gap. In this type of model it may be possible to produce quasi-stationary sparks which drift around the polar cap ($\underline{E} \times \underline{B}$ drift) and ultimately lead to drifting subpulses.

C) Radio Emission

The momentum distribution of accelerated particles is not known but it has been suggested that it consists of primary and secondary particles (particles accelerated through the full potential and electron positron pairs, respectively) with distribution shown below:

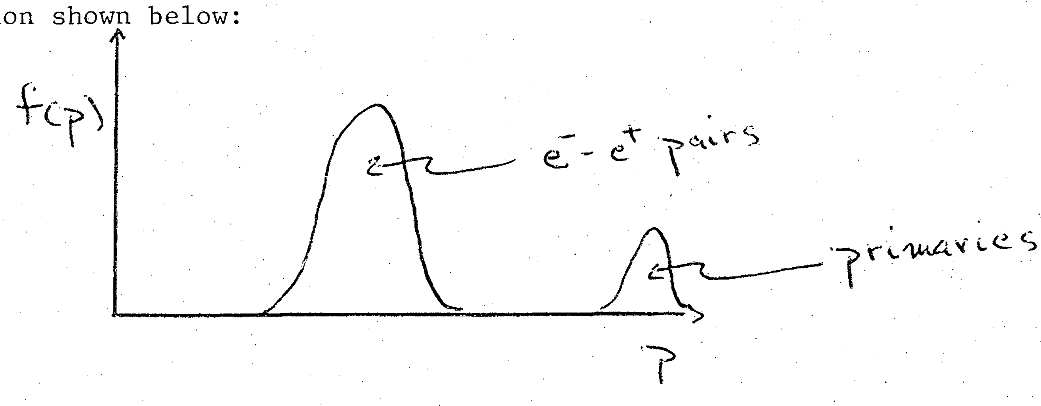

Such a particle distribution is unstable to electrostatic waves which can bunch the particles and lead to the generation of coherent curvature radiation and is unstable to cyclotron waves. Both of these mechanisms enhance emission at the local plasma frequency and could lead to the observed radio emission.

D) Polarization

1) Optical depth effects at self-absorption point.
linear polarization rotates 90 degrees
circular polarization changes sense of rotation

2) Charge imbalance of different sign in different locations.
circular polarization changes sense of rotation

3) Velocity shear at high altitudes can lead to similar effects.

E) Aberration and Photon Flight Time

If emission is to be in phase at different frequencies then emission must be produced at the same altitude in the magnetosphere. Emission at higher altitudes is beamed in the forward direction by aberration. This can be countered by bending of the magnetic field in the backward direction (shearing of field and velocity at high altitude). The finite flight time of photons across any emission region causes photons emitted at a lower altitude to lag (as seen by an observer) photons emitted at a higher altitude. This produces an effect similar to aberration.

The observed phasing of pulsed emission at different frequencies from the Crab and Vela pulsars may be explained by evolution of three different emission mechanisms, γ-rays produced at the surface, radio emission produced above the surface, and synchrotron emission generated near the light cylinder to produce the optical emission (Crab pulsar synchrotron might be responsible for optical, x-ray and γ-ray emission as continuous spectrum).

REFERENCES

(Note: This is far from an exhaustive listing; a few representative articles on the topics mentioned in the lecture are listed. Especially included are some articles which post-date the Groth and Manchester review articles)

Review articles

Groth, E.J. (1975) in "Neutron Stars, Black Holes, and Binary X-ray Sources", Gursky and Ruffini, eds. (Reidel)

Manchester, R.N. (1974) in "Galactic and Extragalactic Radio Astronomy", Verschuur and Kellerman, eds. (Springer-Verlag)

Ginzburg, V.L. and Zheleznyakov, V.V. (1975), Ann. Rev. Astro. Astrophys. 13, 511.

Ruderman, M. (1972), Ann. Rev. Astro. Astrophys. 10, 427.

Hewish, A. (1970), Ann. Rev. Astro. Astrophys. 8, 265.

Pulse Morphology

Manchester, R.N. (1971), ApJ Suppl #199, 23, 283. (average polarization)

Taylor, J.H., Manchester, R.N, Huguenin, G.R. (1975), ApJ 195, 513. (single pulses)

Manchester, R.N., Taylor, J.H., Huguenin, G.R. (1975), Ap.J. 196, 83. (single pulses)

Helfand, D.J., Manchester, R.N., Taylor, J.H. (1975), ApJ 198, 661. (mean profile stability

Rickett, B.J., Hankins, T.H., Cordes, J.M. (1975) ApJ 201, 425. (micropulses)

Ferguson, D.C., Graham, D.A., Jones, B.B., Seiradakis, J.H., Wielebinski, R. (1976), Nature 260, 25. (micropulses)

Pulsars Searches

Davies, J.G., Lyne, A.G., Seiradakis, J.H. (1973), Nature 244, 84.

Large, M.I., Vaughan, A.E. (1971), MNRAS 151, 277.

Hulse, R.A., Taylor, J.H. (1975), ApJ 201, L55.

PSR 1913+16 (Binary)

Hulse, R.A., Taylor, J.H. (1975), ApJ 195, L51.

Taylor, J.H., Hulse, R.A., Fowler, L.A., Gullahorn, G.E., Rankin, J.M. (1976), ApJ 206, I

Observational Methods

Hankins, T.H. and Rickett, B.J. (1975), "Methods in Computational Physics", Vol. 14 (Academic Press). (also discusses microstructure results)

List of Known Pulsars and Their Parameters

Taylor, J.H. and Manchester, R.N. (1975), AJ 80, 794.

Surface Binding Energy

Flowers, Lee, Ruderman, Sutherland, Hillebrandt & Muller 1977, Ap.J., **215**, 291.

Magnetospheres

Ruderman & Sutherland 1975, Ap.J., **196**, 51.

Cheng & Ruderman 1977, Ap.J., **214**, 598.

Fawley, Arons & Scharleman 1977, Ap.J., **217**, 227.

Scharleman, Arons & Fawley 1977, Ap.J., **222**, 297.

Emission & Plasma Stability

Roberts, D.H. and Sturrock, P.A. (1973), ApJ **181**,161.

Benford 1975, Ap.J., **201**, 419.

Benford & Buschauer 1977, MNRAS, **179**, 189.

Hardee & Rose 1974, Ap.J. Letters, **194**, L35.

Hardee & Rose 1976, Ap.J., **210**, 533.

Hardee & Rose 1978, Ap.J., **274**, 219.

Hardee 1977, Ap.J., **216**, 873.

Cheng & Ruderman 1977, Ap.J., **212**, 537.

Cheng & Ruderman 1977, Ap.J., **216**, 865.

Kawamura & Suzuki 1977, Ap.J., **217**, 832.

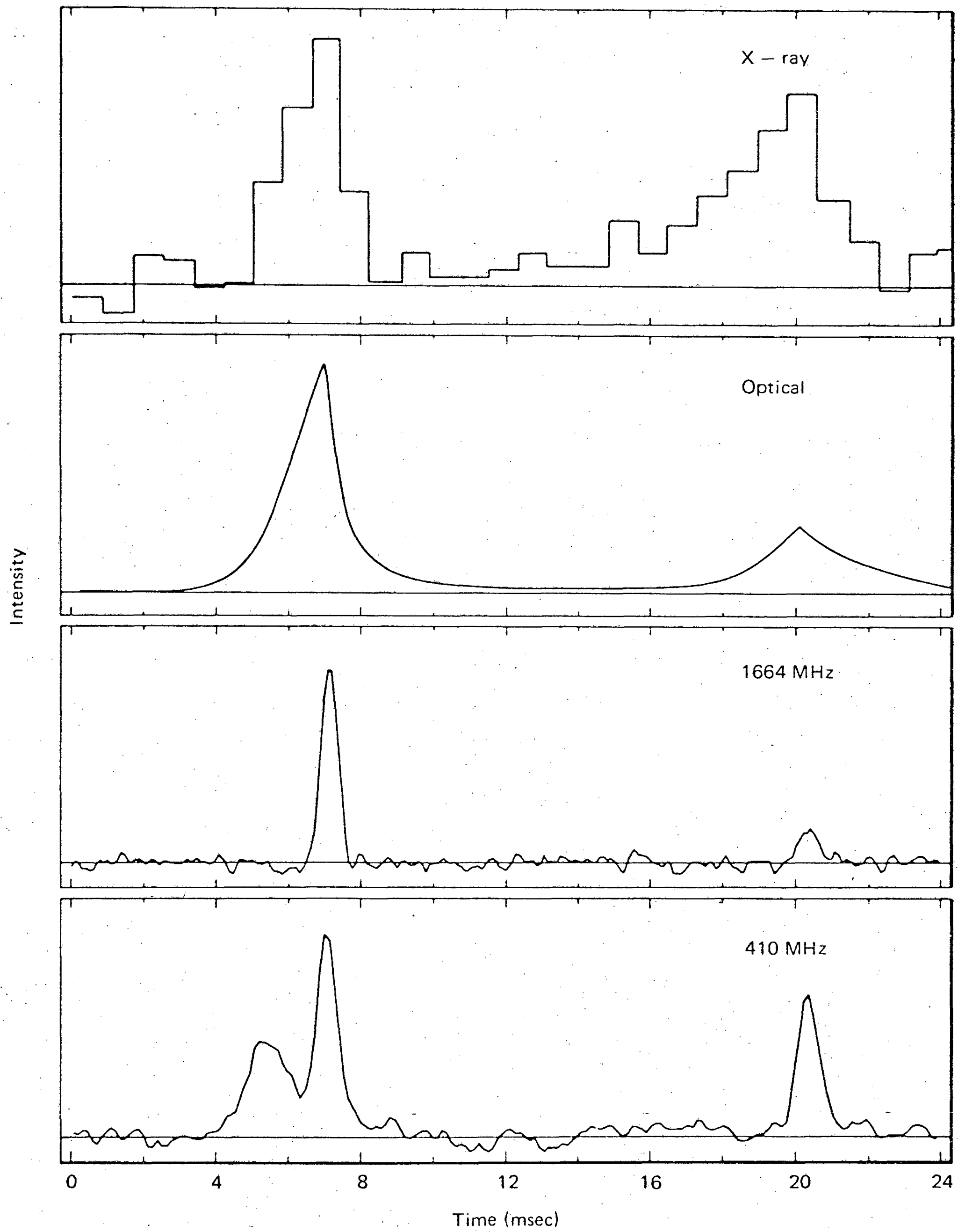

Integrated pulse shapes for the Crab pulsar PSR 0531 + 21 at radio, optical, and X-ray frequencies.

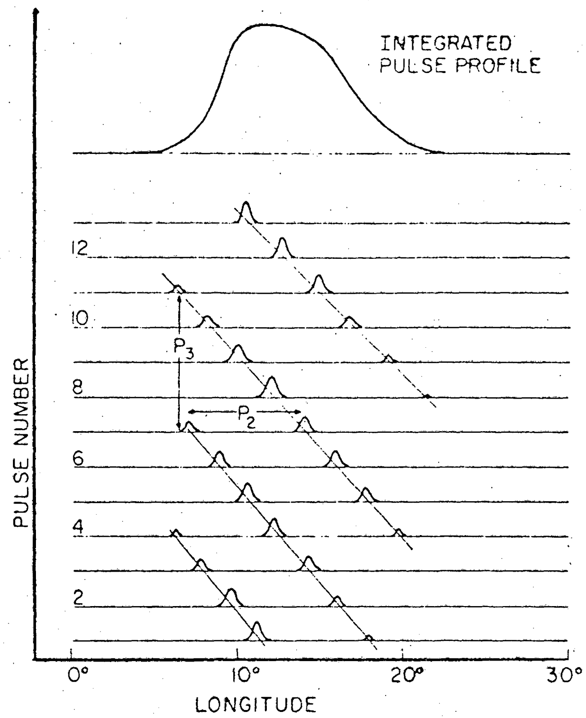

Schematic (after Backer 1973) of integrated pulse profile, arrival times of individual pulses, and definition of P_2, P_3 for those pulsars showing the "drifting subpulse" phenomenon.

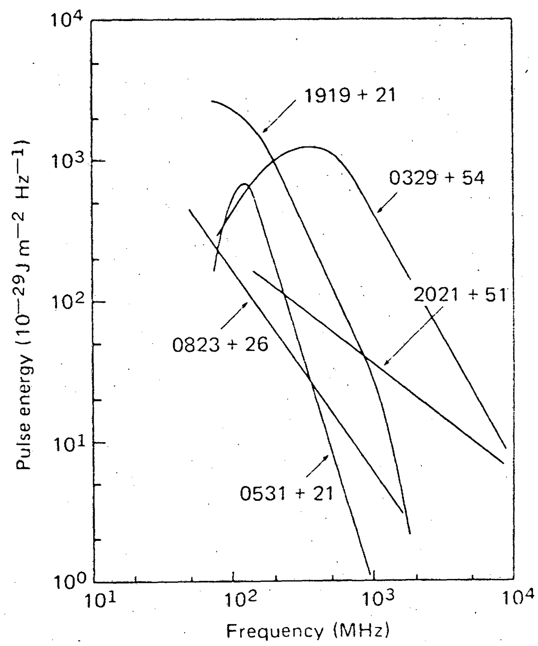

Radio-frequency spectra for several pulsars showing that most pulsars are weak at high frequencies. In some cases there is also a low-frequency turnover.

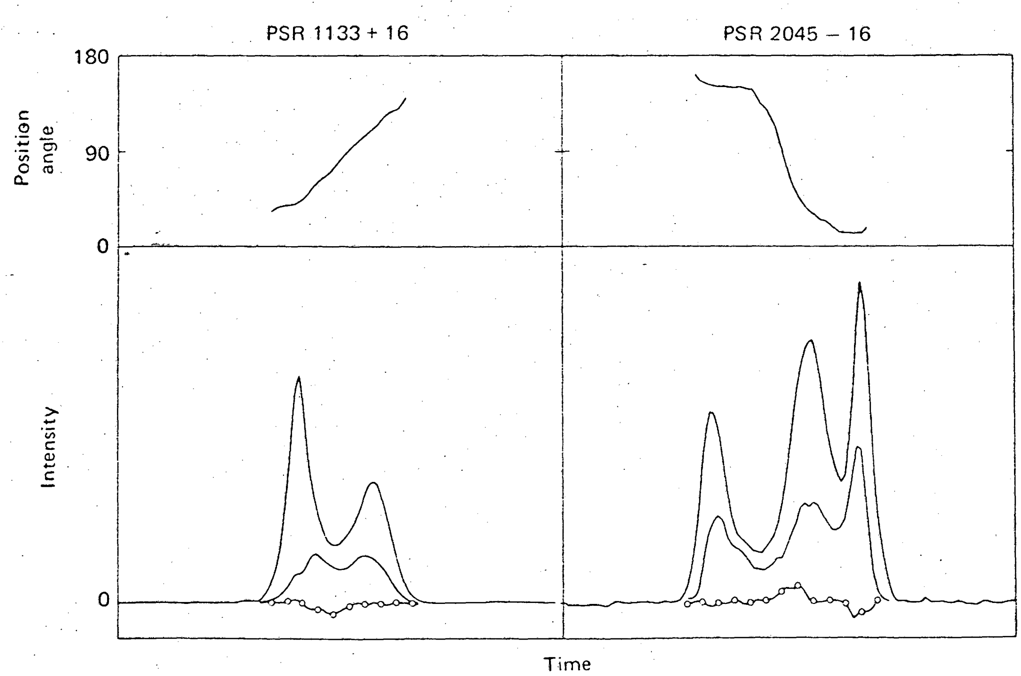

Integrated profiles and polarization parameters for two pulsars PSR 1133+16 and PSR 2045−16. In the lower part of the figure the upper line gives the pulse profile, the second line is the linearly polarized component, and the line with small circles is the circularly polarized component.

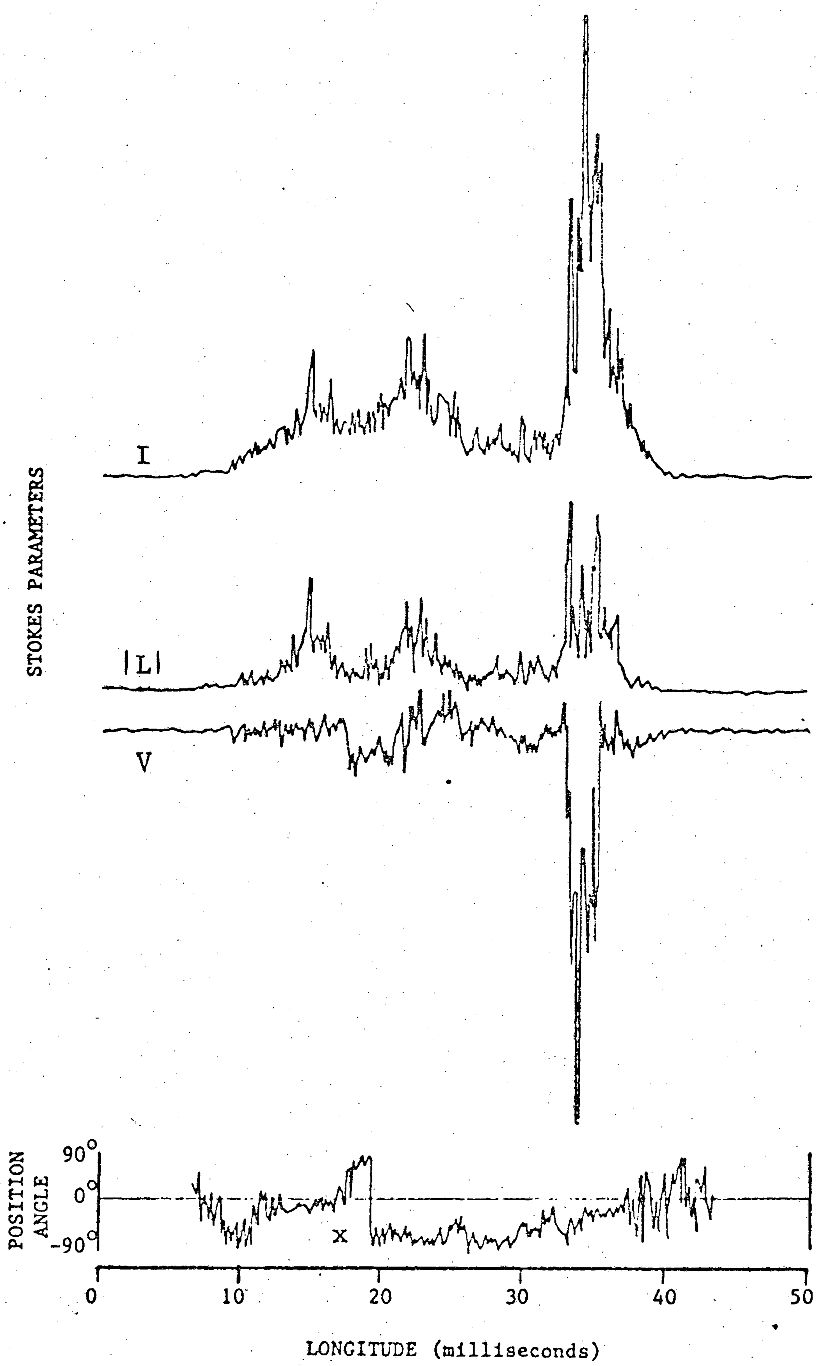

An amorphous pulse with strong emission in the saddle region; a 90° rotation in the position angle (PA) occurs at x where two subpulses overlap.

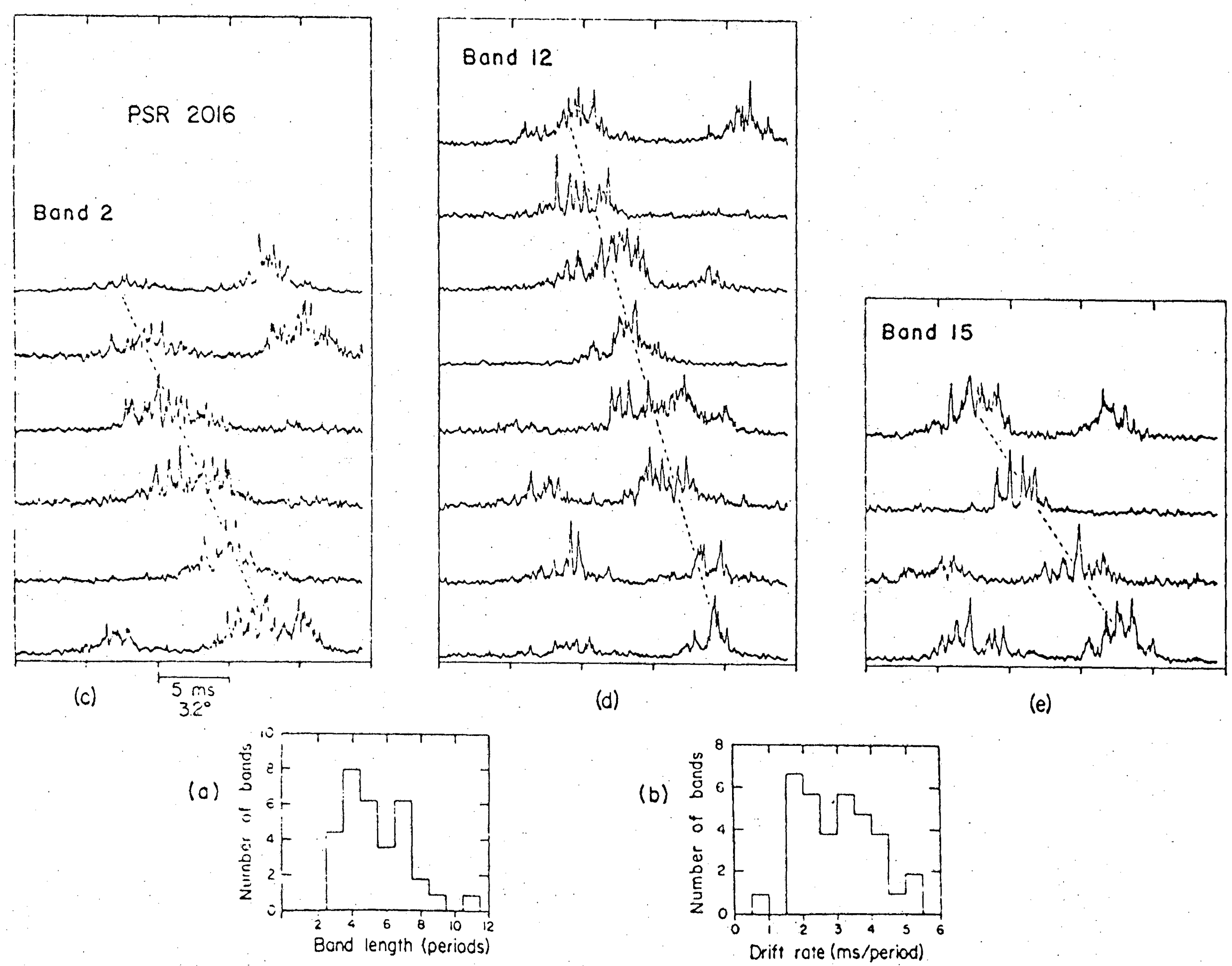

Figure 1 a Histogram of numbers of pulses in drifting subpulse bands.
b Histogram of subpulse drift rates.
c,d,e Pulses of bands 2, 12, and 15 (dashed lines) obtained at 430 MHz. Dispersion distortion has been removed and post-detection smoothing is 100 μs. All pulses are plotted with the same height in order that microstructure be discernible.

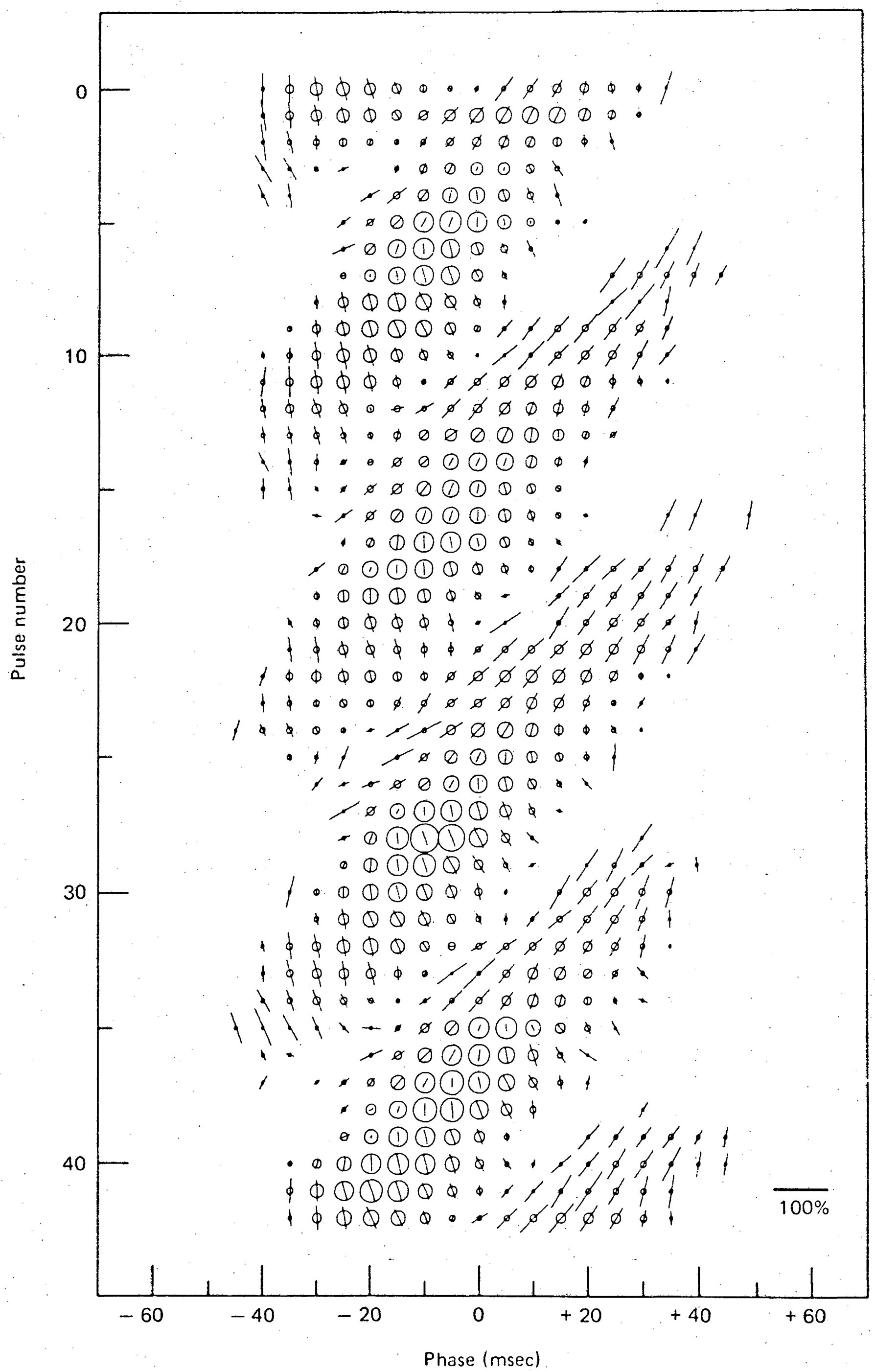

A phase-time diagram for PSR 0809+74 showing the polarization of individual subpulses. At each point, intensity is represented by the circle diameter, percentage polarization by the length of the line, and position angle by the orientation of the line. (Taylor *et al.*, 1971. *Astrophys. Lett.* 9: 205.)

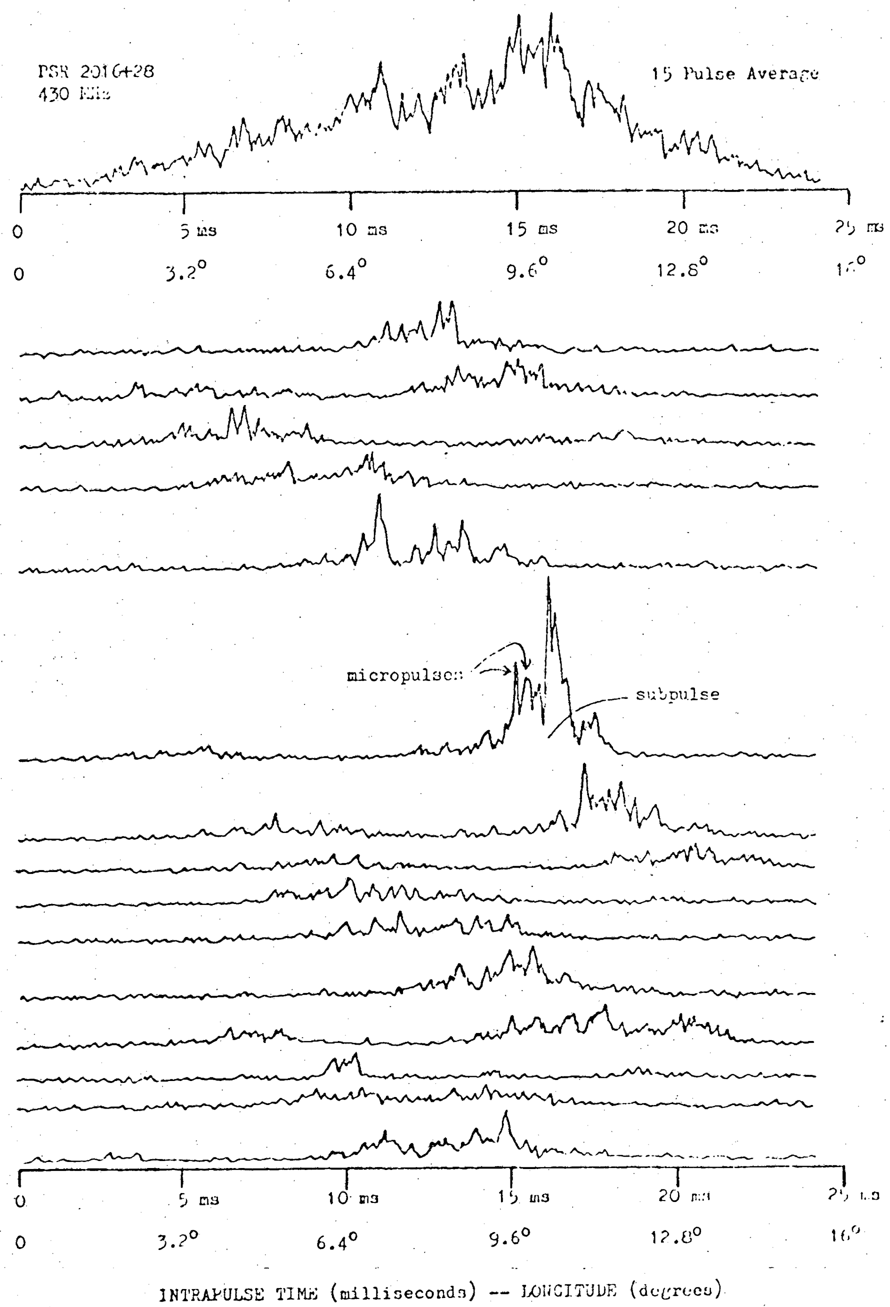

A sequence of pulses from PSR 2016+28 at 430 MHz.

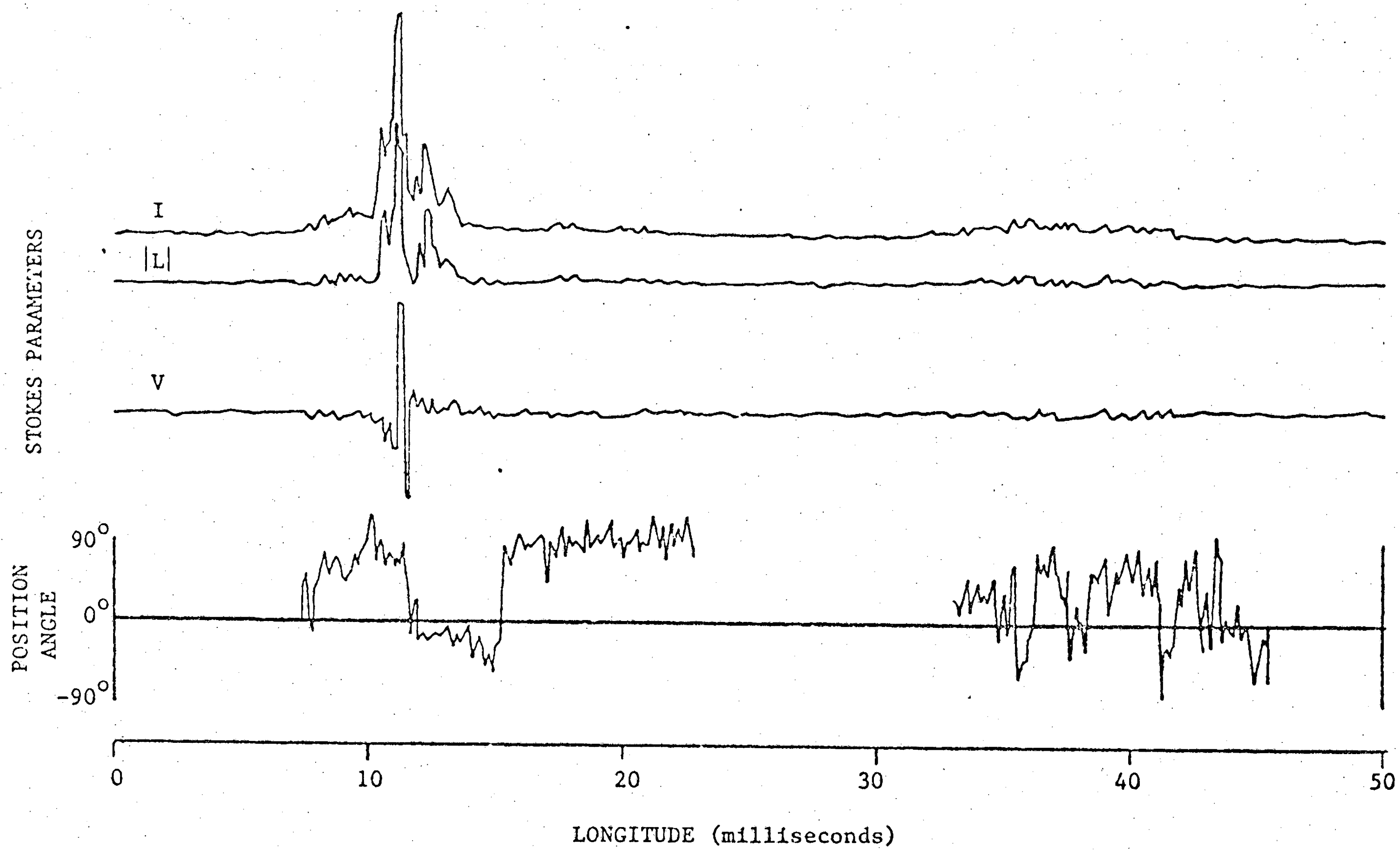

A spiked pulse with a flip of 90° in PA and a change in sense of the circular polarization where micropulses adjoin.

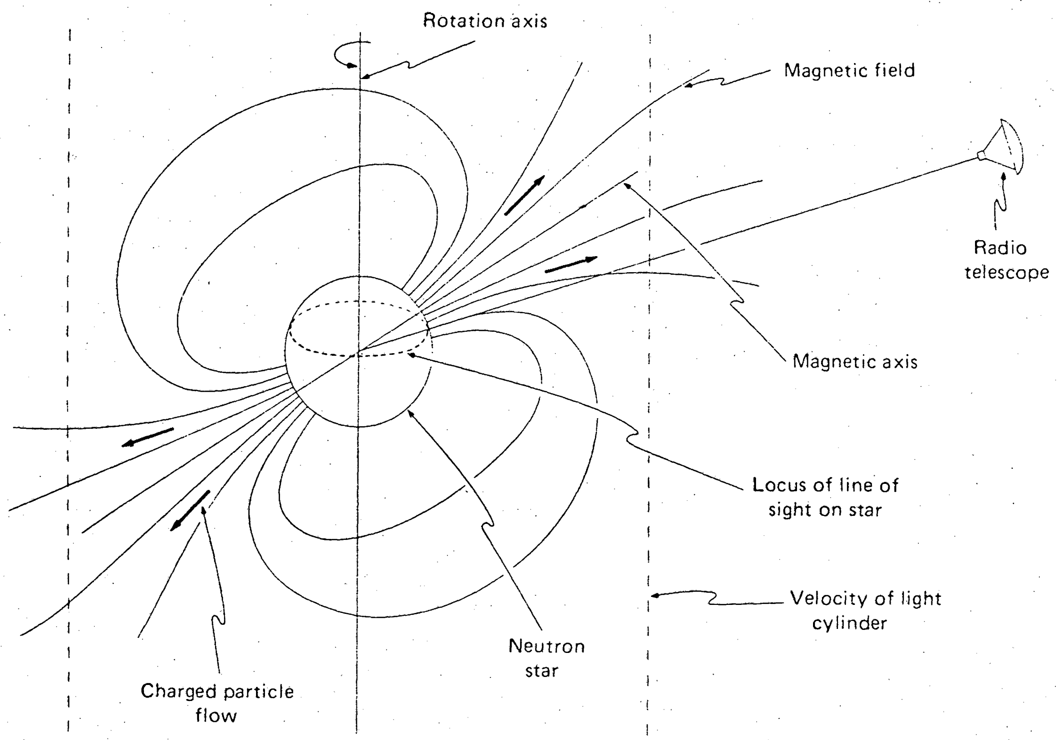

Schematic diagram of the oblique-rotator model for pulsars. Charged particles are thought to stream out from the magnetic poles along those field lines which pass through the light cylinder.

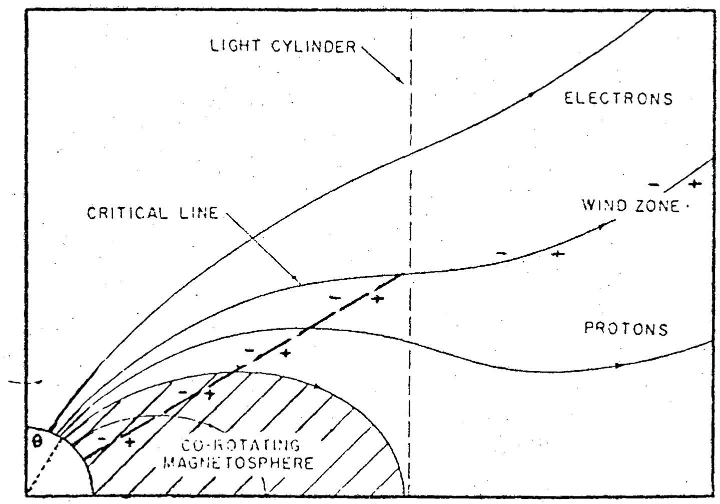

Schematic diagram showing the corotating magnetosphere and the wind zone. Star is at lower left. (Goldreich and Julian 1969)

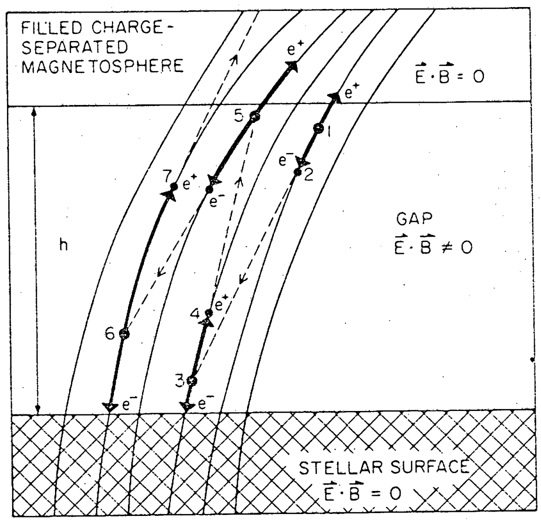

—Breakdown of the polar gap. The solid lines are polar field lines of average radius of curvature ρ; for a pure dipole field $\rho \sim (Rc/\Omega)^{1/2} \sim 10^8 P^{1/2}$ cm, but for a realistic pulsar one expects $\rho \sim 10^6$ cm if many multipoles contribute near the surface. A photon (of energy $> 2\,mc^2$) produces an electron-positron at *1*. The electric field of the gap accelerates the positron out of the gap and accelerates the electron toward the stellar surface. The electron moves along a curved field line and radiates an energetic photon at *2* which goes on to produce a pair at *3* once it has a sufficient component of its momentum perpendicular to the magnetic field. This cascade of pair production—acceleration of electrons and positrons along curved field lines—curvature radiation—pair production results in a "spark" breakdown of the gap.

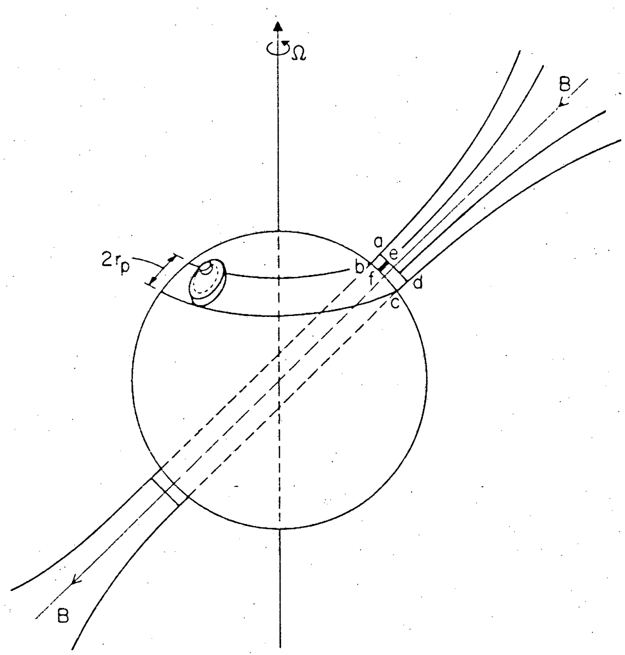

—Schematic of a rotating neutron star with dipole moment somewhat inclined to the rotation axis. The polar cap, of base diameter $2r_p$, moves at fixed latitude. A spark *ef* in the gap *abcd* drifts counterclockwise on a circular path (*dashed line*) on the polar cap centered on the magnetic field axis. This spark feeds relativistic particles onto field lines: coherent microwave radiation is produced tangentially to these field lines far above ($\sim 10^8$ cm) the stellar surface.

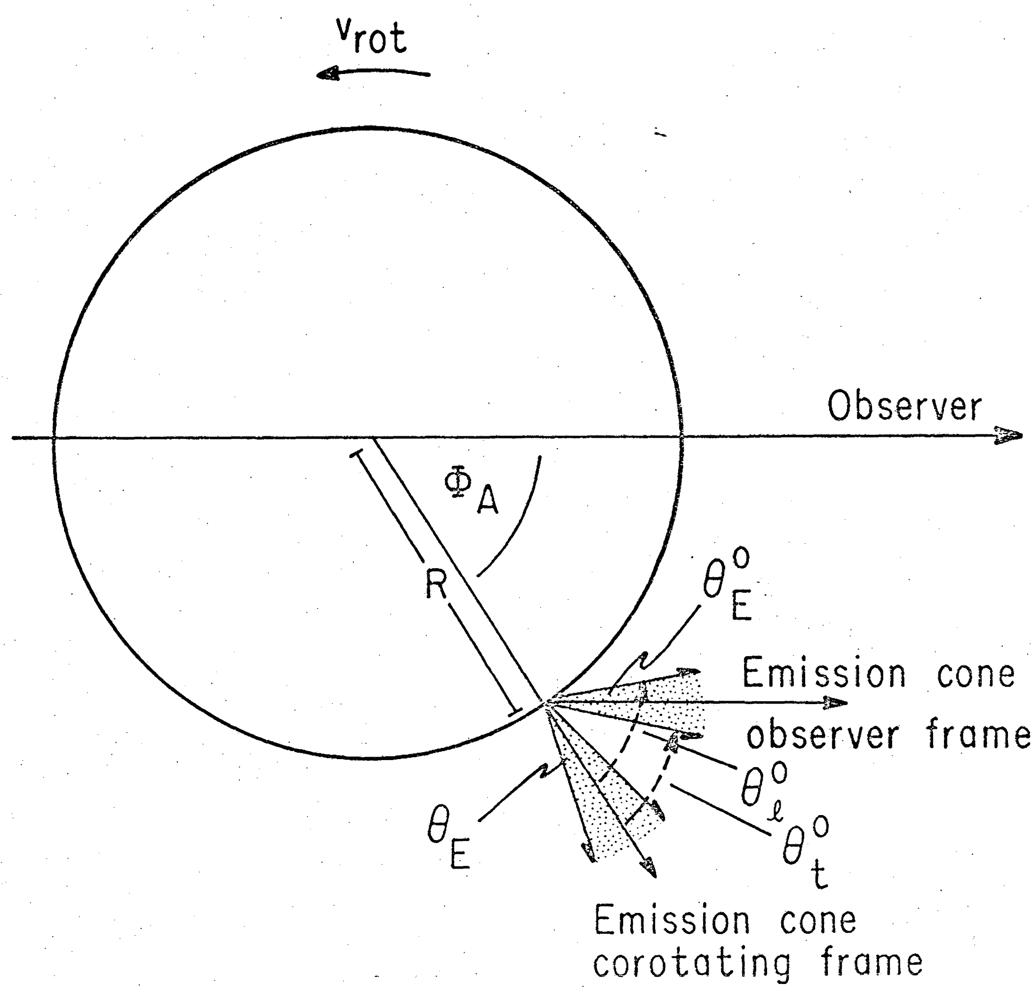

Aberration and beaming of radiation from a rotating source. The angle of aberration is Φ_A and the emission is beamed to the observer in a cone of angular extent θ_E^o which is less than the angular extent θ_E of the emission cone in a frame of reference corotating with the source.

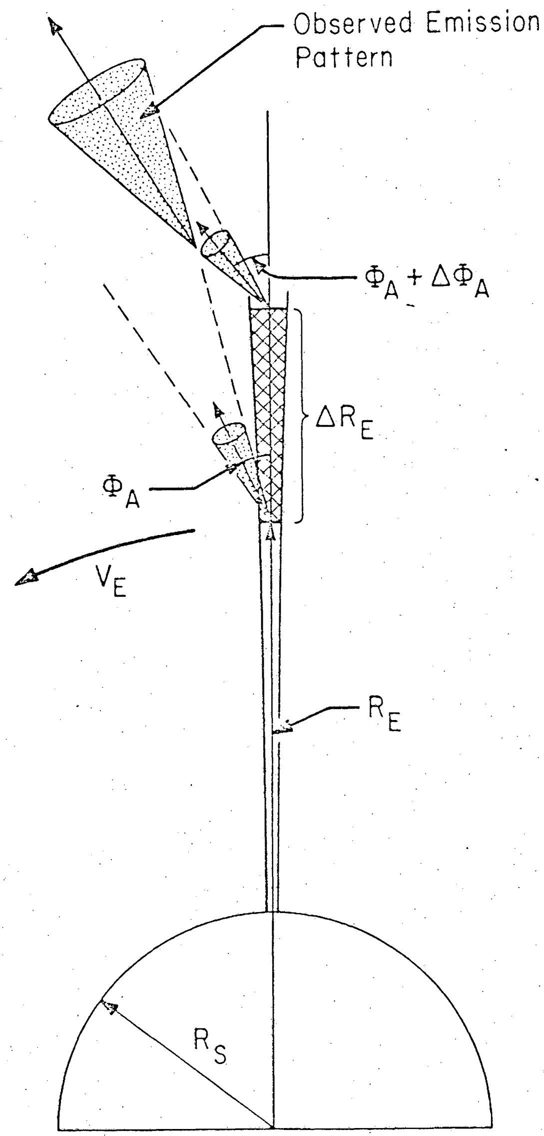

Observed emission pattern produced by aberration when $\Delta\Phi_A >> \theta_E$. The additional effect due to the finite flight time of a photon across ΔR_E is taken into account by replacing Φ_A with $\Phi_A - \Delta\theta$ at the bottom of the emission region.

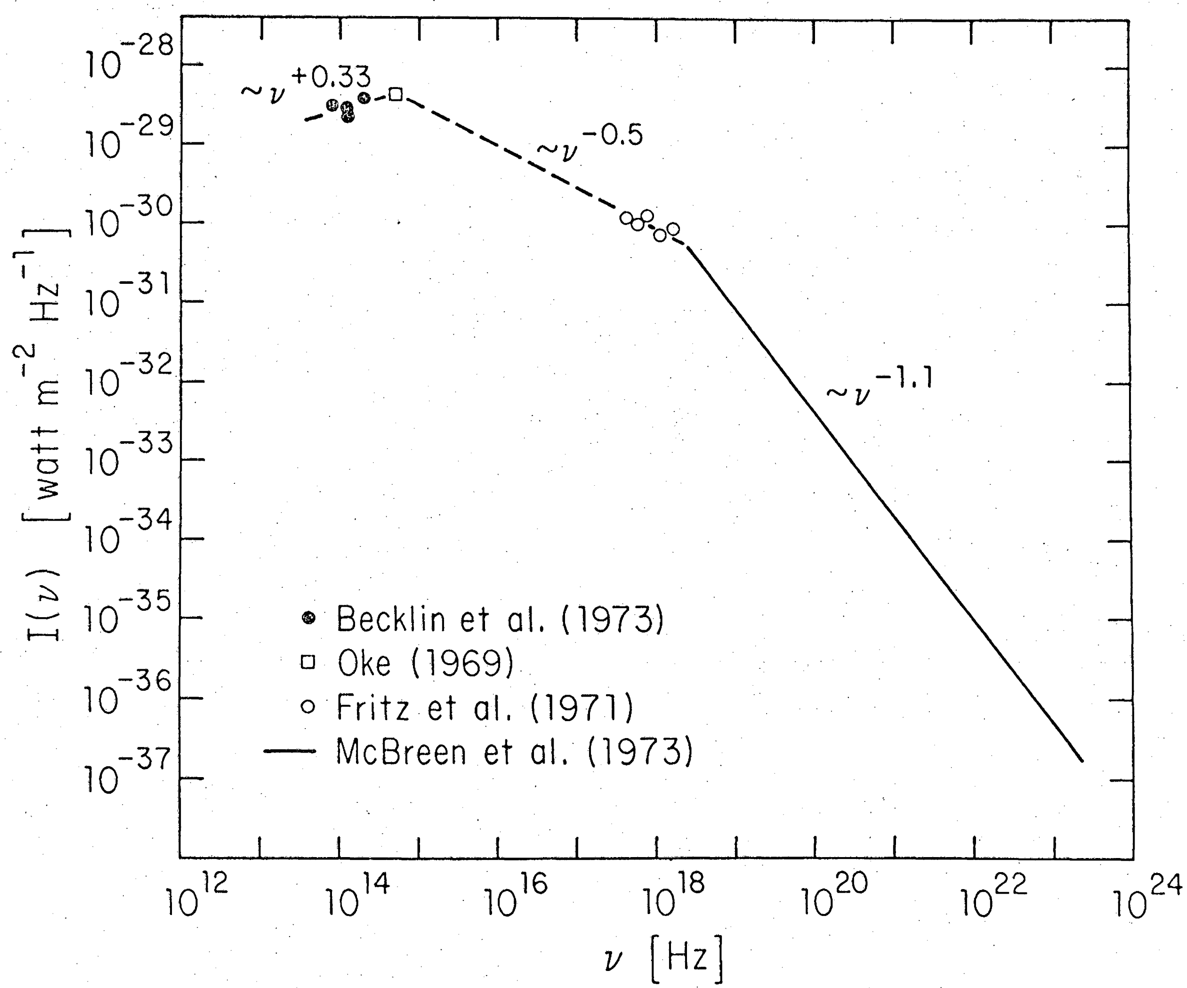

Approximate fit to the pulsed intensity from the Crab pulsar by a continuous spectrum with three spectral indicies.

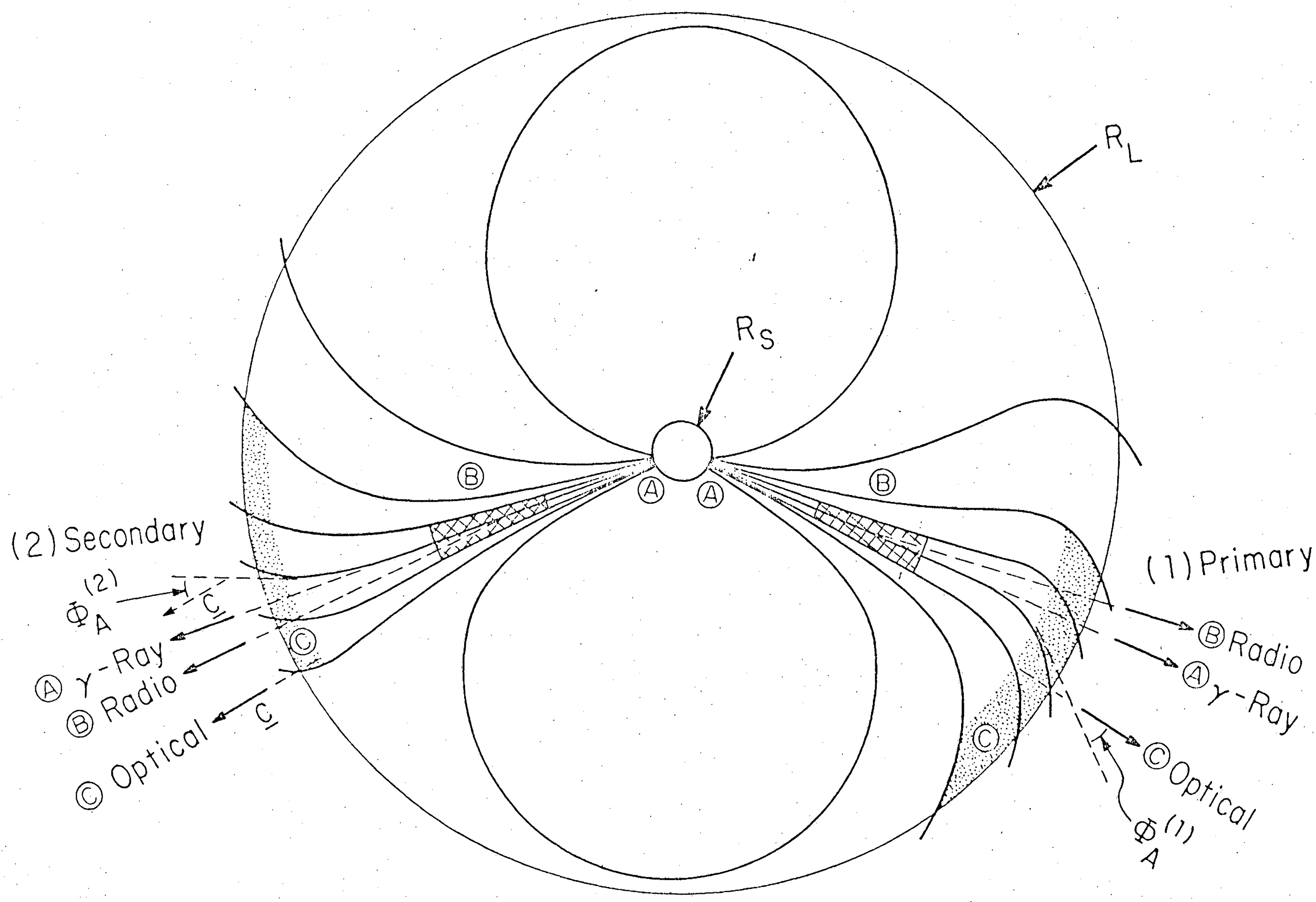

Configuration of magnetic field and emission regions leading to difference in phase between pulsed emission at different frequency.

Aberration $\Phi_A^{(1)}$ is not enough to overcome the magnetic field shearing near the light cylinder and hence the primary optical pulse trails the primary γ-ray pulse. However, $\Phi_A^{(2)}$ is sufficient to cause the secondary optical pulse to preceed the secondary γ-ray pulse.